PCCP

Accepted Manuscript

ROYAL SOCIETY OF CHEMISTRY

www.rsc.org/pccp

Time-resolved spectroscopy of the singlet excited state of betanin in aqueous and alcoholic solutions

Monika Wendel,[a] Stanislaw Nizinski,[a] Dorota Tuwalska,[b] Karolina Starzak,[b] Dominika Szot,[b] Dorota Prukala,[c] Marek Sikorski,[c] Slawomir Wybraniec,[b] and Gotard Burdzinski*[a]

Abstract

Photophysical properties of betanin in aqueous and alcoholic solutions were determined at room temperature using ultrafast UV-vis-NIR transient absorption spectroscopy (λ_{exc} = 535 nm). Its S_1 absorption bands appear with the maxima at about $\lambda \sim 450$ and 1220 nm. The short betanin S_1 state lifetime (6.4 ps in water) is mainly determined by the efficient $S_1 \rightarrow S_0$ radiationless relaxation, probably requiring a strong change in geometry, since the S_1 lifetime grows to 27 ps in the more viscous ethylene glycol. The fluorescence quantum yield is very low ($\Phi_f \sim 0.0007$ in water), therefore this deactivation path is of minor importance. Other processes, such as $S_1 \rightarrow T_1$ intersystem crossing or photoproduct formation, are virtually absent, since full $S_0 \leftarrow S_1$ ground state recovery is observed within tens of picoseconds after photoexcitation. The observed fast light-to-heat conversion in the absence of triplet excited state formation supports the idea that betanin is a photoprotector *in vivo*.

Introduction

Betanin, (**bn**, Figure 1) known for its applications in the pharmaceutical, cosmetic and food industries as a red pigment (E-number E162),[1, 2] is one of the best known betacyanin dyes occurring in a few plant families belonging to the Caryophyllales.[3] The presence of **bn** in leaves, fruits, roots, stems, and flower petals results in a characteristic red/purple color attractive to pollinators. Accumulation of betacyanins in response to white and UV light has been observed in light-stressed stems of cacti species[4] and *Mesembryanthemum crystallinum* L.,[2, 5, 6] indicating that betacyanins probably act as photoprotectors in living tissues. Furthermore, **bn** may contribute to the protection from the oxidative damage in plants and foods, since quenching of singlet oxygen ($^1O_2$) by **bn** has been reported in aqueous solutions.[7] Dye-sensitized solar cells based on **bn** exhibit a remarkably high energy conversion efficiency (2.7 %)[8] for a natural dye sensitizer; two-electron dye oxidation following one-photon excitation has been recently proposed.[9] Red beet *Beta vulgaris* L.[10, 11] as well as fruits of some cacti species of *Opuntia*,[12] *Mammillaria*[13] and *Hylocereus*[14] contain **bn** dye (100 - 600 mg kg^{-1} in red beet).[11] Pure **bn** can be obtained by purification of plant extracts.[15]

Insert Figure 1

The structure of **bn** in aqueous solution has been investigated by NMR spectroscopy, quantifying a 80:20 mixture of the *E*/*Z* stereoisomeric forms (isomerization at C(12)=C(13), Figure 1).[16] Typically **bn** shows good solubility in water and alcohols.[17, 18] Aqueous solutions of **bn** are stable in the pH range from 3.5 to 7;[17, 19] however, high temperature, light, metal cations and oxygen reduce the dye stability.[20] Temperature is the main factor causing **bn** chemical decay, at low temperatures light-induced degradation may also be important.[20] The mechanism of photodegradation remains unclear, a first-order reaction was observed for **bn** in aqueous solution at T < 25°C.[21] Its photodegradation apparently involves molecular oxygen, becoming undetectable in anaerobic conditions.[21] Dehydrogenated and decarboxylated betanins were the main photoproducts in aqueous solutions formed upon UV irradiation.[22] A weak **bn** fluorescence has been recently reported with the maximum at 620 nm upon excitation at λ_{exc} = 535 nm.[8, 18] The absorption band of **bn** is quite strong, its molar extinction coefficient is ε(536 nm) = 65000 $M^{-1}cm^{-1}$.[18, 23] DFT and TDDFT calculations have been performed for **bn**,[24, 25] predicting a strong $\pi \rightarrow \pi^*$ electronic transition, with the energy close to the experimental values.[26] Following the optical transition, the electron density shifts from the benzene ring to the dihydropyridine moiety.[24] To the best of our knowledge, in contrast to

structurally close betaxanthins,[27] time-resolved spectroscopy has never been used in studies of **bn** photophysics and photochemistry in solutions. Our current objective is to describe the properties of betanin in the S_1 excited state and characterize the S_1 state deactivation paths.

Results and Discussion

Stationary UV-vis absorption and fluorescence

Stationary UV-vis absorption spectra of **bn** reveal a band with the maximum at about $\lambda_{abs}^{max} \sim 535$ nm in aqueous and alcoholic solutions (Figure 2).

Insert Figure 2

This band corresponds to the $S_0 \rightarrow S_1(\pi,\pi^*)$ electronic transition, according to literature[24, 25] and our time-dependent density functional theory (TD-DFT) calculations (Tables S1, S2 in the Supporting Information). The fluorescence spectra recorded for **bn** in water with the excitation at $\lambda_{exc} = 530$ nm have a maximum at about $\lambda \sim 640$ nm, in line with previous reports.[8, 18] The **bn** fluorescence excitation spectrum agrees well with the stationary UV-vis absorption spectrum (Figure S1). We determined the fluorescence quantum yield Φ_f of **bn** in solution, using rhodamine 6G in water as a reference ($\Phi_f^{ref} = 0.9$).[28] The fluorescence quantum yield for **bn** in water is a considerably low value ($\Phi_f = 0.0007$) in agreement with the results of Knorr et al. ($\Phi_f \sim 0.001$),[9] and explaining why **bn** had been considered non-fluorescent in the past.[29] The Φ_f increases by the factor of three when using ethylene glycol instead of methanol (Table 1), the S_1 state being thus sensitive to solvent viscosity.[30] Similar sensitivity to solvent viscosity has been observed for the structural counterparts of **bn** - betaxanthin dyes.[27] Betanin is insoluble in viscous linear alcohols, such as 1-decanol or 1-pentanol. The stationary spectra of **bn** in comparison to indicaxathin[27] show larger Stokes shifts (2900 vs. 1270 cm^{-1} in water, 2400 vs. 1050 cm^{-1} in methanol), implying a substantial increase of the dipole moment of **bn** in the S_1 state.

Insert Table 1

Broadband UV-vis-NIR transient absorption

Broadband UV-vis-NIR transient absorption spectroscopy was used for characterization of the **bn** S_1 state properties and dynamics in water. The excitation wavelength was set at λ_{exc} = 535 nm, tuned to the $S_0 \rightarrow S_1(\pi,\pi^*)$ electronic transition (Table S1) and close to the maximum of the **bn** stationary absorption.

Insert Figure 3

Both positive and negative transient absorption bands were observed (Figure 3) at the initial time delays. They are interpreted as follows: the positive bands at 450 and 1225 nm (7:1 signal amplitude ratio) are assigned to **bn** in the S_1 state, the negative bands peaking at about 535 and 670 nm are attributed to S_0 depletion and $S_1 \rightarrow S_0$ stimulated emission, respectively. The spectral shapes of the negative bands are similar to those of the **bn** UV-vis ground-state absorption and the scaled fluorescence spectrum (multiplied by λ^4)[31], respectively (Figure 3). These negative signal contributions cannot affect the S_1 state absorption at 1225 nm. To retrieve the S_1 excited state lifetime, the band integral over 330–1345 nm was calculated, according to the equation $BI(t) = \int_{330}^{1345} \Delta A(t,\lambda) \frac{d\lambda}{\lambda}$, and the kinetics $BI(t)$ was fitted with a single-exponential function, resulting in τ_{S1} = 6.4 ps (Figure 4).

Insert Figure 4

Note that analysis of the band integral can minimize potential contributions from vibrational relaxation (VR).[32] Although NMR structural investigation revealed the presence of two stereoisomeric forms (ratio 80:20) of **bn** in the S_0 ground state,[16] our band integral decay was fitted very well with a single-exponential function. Possibly, the two stereoisomeric forms are initially photoexcited to their respective S_1 singlet excited states, the latter being characterized by very similar decay dynamics. Global analysis produced two characteristic time constants: τ_1 = 0.86 and τ_2 = 6.8 ps (Figure S2). Note that the longer component τ_2 is similar to τ_{S1}. The main contribution to the shorter time-constant τ_1 comes from the solvation of the S_1 state, since a similar red shift within the 3 ps time window is observed for both the stimulated emission and the S_1 NIR absorption bands (Figure 3).

Another possible reaction occurring within the picosecond time frame is the vibrational cooling that is dissipating the energy from the hot chromophore to the solvent molecules. This process may occur after **bn** photoexcitation to the S_1 state, or for vibrationally

excited S_0 generated in $S_1 \rightarrow S_0$ internal conversion.[33] Note that vibrational cooling is typically manifested by a narrowing of the hot S_1 or S_0 absorption bands, or fluorescence bands.[32, 34-36] The excess of vibrational energy in the **bn** S_1 state due the additional excitation energy at λ_{exc} = 475 vs. 535 nm has a small influence on the transient absorption spectra and the deduced decay-associated spectra (Figures S2 and S3). A substantial excess of the vibrational energy can be expected in the nascent **bn** S_1 state when using UV excitation (λ_{exc} = 287 nm). Upon UV excitation, the initially formed set of highly excited singlet states (S_n, n>1, Table S1) undergoes $S_n \rightarrow S_1$ internal conversion. The rise of the S_1 absorption band peaking at λ_{max} = 450 nm follows the appearance of the bleaching band (Figure 5), with the apparent rate limited by the instrument response function (350 fs).

Insert Figure 5

Close inspection of the spectrum associated with the fast component (0.88 ps, Figure 5B) reveals a smaller decay of the transient absorption signal in the central part (at about 465 nm) compared to the decay in the blue (<465 nm) or red (>465 nm) wings, caused by a weak S_1 absorption band narrowing, in addition to a gentle red-shift of the spectra (solvation, Figure S4). This fast vibrational cooling manifested by band-narrowing (~0.88 ps) proceeds in parallel to solvation.

The negative band at about $\lambda \sim 535$ nm in the transient absorption spectra (Figure 3) is due to the **bn** ground state bleaching, with the differential molar absorption coefficient $\Delta\varepsilon(535nm) = \varepsilon_{S1}-\varepsilon_{S0} \sim -65000\ M^{-1}\ cm^{-1}$. This conclusion is supported by (1) the shape of the S_0 bleaching band similar to that of the stationary **bn** absorption band and (2) the high value of $\Delta\varepsilon(520nm) = \varepsilon_{S1}-\varepsilon_{S0} = -78000 \pm 20000\ M^{-1}cm^{-1}$ estimated from comparative actinometric measurements using $Ru(bpy)_3^{2+}$ as a reference compound (Figure S5). In order to estimate the molar absorption coefficient $\varepsilon_{S1}(450nm)$ of **bn** in the relaxed S_1 state, we used the singlet depletion method, with the relation

$$\Delta A_{6ps}(450nm)/\Delta A_{6ps}(535nm) = (\varepsilon_{S1}(450nm) - \varepsilon_{S0}(450nm))/\Delta\varepsilon(535nm),$$

where $\varepsilon_{S0}(450nm) = 7175\ M^{-1}cm^{-1}$, while the values $\Delta A_{6ps}(450nm)$ and $\Delta A_{6ps}(535nm)$ were taken from Figure 3. The deduced $\varepsilon_{S1}(450nm) = 66000\ M^{-1}cm^{-1}$ characterizes the **bn** S_1 state absorption band maximum in water.

Our analysis of the transient absorption data obtained for **bn** in methanol reveals a very similar spectral shape and dynamics (Figure S6A). The replacement of methanol by a more viscous ethylene glycol has little influence on the spectral band locations (Figure S6B),

though it causes an extension of the **bn** S_1 state lifetime to 27 ps (Figure 4). The increase in the **bn** S_1 state lifetime with solvent viscosity matches a similar trend observed for the fluorescence quantum yields (Table 1). The shorter characteristic time constant τ_1 = 4.4 ps retrieved from global analysis (Figure S2) in ethylene glycol is longer in comparison to those determined in methanol (1.6 ps) or water (0.86 ps), as expected for solvation, since the viscosity affects the diffusive solvent motion.[37]

We performed additional experiments on red beet aqueous extracts (*Beta vulgaris* L.). It is known that **bn** is the dominant pigment in the extract;[38-40] the 535 nm excitation is selective for **bn**, since the betaxanthin absorption band is located at shorter wavelengths (λ_{max} ~ 480 nm).[19] The transient absorption spectra and dynamics (Figure S7) are very close to those for pure **bn** in water (Figures 3 and S2A). We also recorded the transient absorption characteristic for **bn** (λ_{exc} = 535 nm) in aqueous extracts from berries of *Phytolacca americana* L. and purple cactus pears of *Opuntia* spp., where **bn** also dominates.[12, 41]

Our results obtained in solution may also be compared to a recent report on **bn** adsorbed on titanium dioxide or zirconium dioxide films.[9] The S_1 dye absorption in these samples also had a maximum at about 450 nm, the S_0 bleaching band was at 530 nm, and the stimulated emission was at about 700 nm. The time-constants obtained in these experiments were quite similar to our results (0.8 and 6 ps on ZrO_2,, photo-oxidation apparently absent), with a larger contribution of the fast component.

Properties of betanin in the S_1 singlet excited state

The photoexcitation of the **bn** solutions with visible light (λ_{exc} = 535 nm) produces **bn** in the S_1 excited state, according to the TD-DFT calculations (Table S1). This S_1 state possesses characteristic absorption bands at ca. 450 and 1220 nm in both aqueous and alcoholic solutions (Figures 3, S6). The corresponding molar absorption coefficients are 66000 and 10500 $M^{-1}cm^{-1}$ in aqueous solution. The determined **bn** S_1 state lifetime (6.4 ps) is short and the fluorescence quantum yield (Φ_f) is low in aqueous solutions, in comparison to those of the structurally similar betaxanthins dyes.[27] In alcoholic solutions, the **bn** S_1 lifetime increases from 7.7 to 27 ps upon the substitution of methanol by the more viscous ethylene glycol. The dependence of the S_1 lifetime on the solvent viscosity suggests a significant change in dye geometry upon the S_1 deactivation. Molecular rotation around the C_{12}=C_{13} bond

may accelerate the internal conversion process. A 80:20 mixture of the *E*/*Z* stereoisomeric forms of **bn** in the S_0 ground state (Figure 1) in aqueous solution has been reported on the basis on NMR results.[16]

One of the most important findings from the ultrafast experiments is the full **bn** ground state S_0 recovery, as the transient absorption spectra reach their baseline level within tens of picoseconds after the photoexcitation (Figures 3, 5 and S6). We therefore conclude that neither the **bn** triplet excited state is generated through the $S_1 \rightarrow T_1$ intersystem crossing, nor photoproducts are formed in noticeable amounts, since at sub-nanosecond delays: (a) the S_0 **bn** bleaching band is absent (b) no new positive absorption bands are observable. These features were reproducibly observed at different excitation wavelengths (535, 475, and 287 nm). Since the fluorescence quantum yield of **bn** are low in aqueous and alcoholic solutions (Table 1), we conclude that the radiationless transition is the main S_1 state deactivation path. A similar of behaviour of **bn** can be expected upon photoexcitation *in vivo.* Indeed, the transient absorption of various aqueous extracts from red beet, berries or purple cactus pears (all possessing **bn** as the dominant dye) show similar transient spectra and dynamics (Figure S7), in comparison to pure **bn** aqueous solutions. Apparently, the confirmed presence of numerous chemical substances in the extracts (including sugars, proteins, vitamins, minerals, and amino acids),[42] does not affect the **bn** photophysics to a noticeable degree.

Upon direct **bn** photolysis, the T_1 state is not formed, its absence excludes sensitization of the toxic forms of oxygen ($^1O_2$) *in vivo*. The efficient light to heat conversion supports the idea that **bn** is a natural photoprotector, in line with other reports showing that it accumulates in living plant tissue in response to exposure to white or UV light.[2, 4-6] Chemical quenching of the singlet oxygen ($^1O_2$) by **bn** has been reported in aqueous solutions,[7] thus **bn** may also contribute to the protection from oxidative damage in plants.

A solvation process was also observed in ultrafast experiments, since the nascent S_1 **bn** absorption and stimulated emission bands all undergo a spectral shift over the time-window of 3 ps in aqueous solutions (Figures 3, S4A). The solvation characteristic time due to the solvent diffusion (~0.9 ps) agrees well with other reports on dyes in water,[37, 43, 44] note that a shorter component of the solvation (<100 fs) attributed to inertial motion of the solvent molecules may also exist; its elucidation, however, requires a better apparatus time resolution. An alternative assignment of the 0.9 ps component involves the dye conformational dynamics,[34] although we are inclined to attribute the observed spectral shift to solvation, for the following reasons: (1) the calculated dipole moment of the ground-state **bn** is quite high

($\mu(S_0)$ = 14 D, at level B3LYP/6-311++g(d,p) PCM = water), while a substantial change in the electronic distribution has been predicted theoretically in the S_1 state;[24] (2) the stationary fluorescence data (Figure 2) show a larger Stokes shift in water in comparison to the less polar methanol (2900 vs. 2400 cm^{-1}); (3) the transient NIR absorption band undergoes a larger spectral shift over the 0.3 - 10 ps time window in water than in methanol (200 vs. 130 cm^{-1}). The solvation effects were less pronounced in our previous study of the structurally similar indicaxanthin,[27] while the Stokes shifts were also smaller (1270 cm^{-1} in water vs. 1050 cm^{-1} in methanol).

Another process, occurring on a similar time scale as solvation, is vibrational relaxation of **bn** in the S_1 state. Observation of this process is facilitated in experiments performed with UV excitation (λ_{exc} = 287 nm, $S_0 \rightarrow S_n$ transition, n>1, Figure 5A). The initially photoexcited **bn** in the S_n state undergoes the subsequent $S_n \rightarrow S_1$ internal conversion, resulting in generation of **bn** in the S_1 state with a substantial excess of vibrational energy. Vibrational cooling is manifested by the S_1 state absorption band-narrowing (~0.88 ps, Figures 5B and S4B). Such short time-constant can be explained by solute-solvent coupling. [32, 35] Indeed, the presence of carboxyl, hydroxyl, and amino groups in **bn** ensures efficient coupling with the solvent by hydrogen bonding. Similarly short time-constants of vibrational cooling have been reported for some molecules (*p*-nitroaniline or 9-methyladenine) in aqueous solutions nascent with a high excess of vibrational energy.[33, 45]

Conclusions

In summary, we present new insights on the photophysics of **bn** in aqueous and alcoholic solutions on the basis of the results obtained with broadband UV-vis-NIR transient absorption and steady-state fluorescence spectroscopies. The S_1 singlet excited state has distinctive absorption bands at ca. 450 and 1220 nm. The **bn** lifetime is very short in solvents of low viscosity (τ_{S1} = 6.4 ps in water). The $S_0 \leftarrow S_1$ internal conversion is the main S_1 state deactivation process, while the $S_1 \rightarrow T_1$ intersystem crossing is virtually absent. The fluorescence is a minor S_1 state deactivation path, confirmed by low fluorescence quantum yields ($\Phi_f \sim 0.0007$ in water). The **bn** S_1 state lifetime shows sensitivity to solvent viscosity, with an extension of τ_{S1} from 7.7 to 27 ps observed upon the change of methanol to ethylene glycol. The efficient light-to-heat conversion indicates the photoprotective role of **bn** in plants. We plan to study other betacyanins in order to establish correlations between their

structure and photophysics. Moreover, the mechanism of $^1O_2$ chemical quenching by betacyanins remains an intriguing issue.

Experimental Section

Betanin was obtained by purification of fruit extract of red *Opuntia ficus-indica* L. Mill received from Italy. The isolation procedure was based on the method of indicaxanthin purification, accomplished by flash chromatography and preparative high-performance liquid chromatography (Supporting Information).[27] Water, alcohols, tris(bipyridine)ruthenium(II) and rhodamine 6G were purchased from Aldrich. All experiments were performed at room temperature.

Femtosecond UV-vis-NIR transient absorption spectra were collected on a commercially available system (Ultrafast Systems, Helios). The ultrafast laser system consists of a short-pulse titanium-sapphire oscillator (Mai-Tai, Spectra Physics, 70 fs) followed by a high-energy titanium-sapphire regenerative amplifier (Spitfire Ace, Spectra Physics, 100 fs). The 800 nm beam was split into two beams to generate: (1) pump (λ_{exc} = 535, 475 or 287 nm) in the optical parametric amplifier (Topas Prime with NirUVis frequency mixer) and (2) probe pulses - white light continuum in UV-vis-NIR (330 – 1370 nm) range by using CaF_2 plate (330 – 660 nm), sapphire (440 – 780 nm) and YAG crystal (830 – 1345 nm). The remaining 800 nm photons in the probe pulse were filtered out before the sample, to avoid signal contribution caused by 800 nm pulse induced stimulated emission in **bn**. The pump pulse energy was typically about 0.5 μJ. The spectral shape and kinetics remained virtually unchanged within the 0.2 – 2.0 μJ excitation laser pulse energy range (Figure S8), and in the 5×10^{-6} – 7×10^{-5} M **bn** concentration range. In most of the transient absorption experiments, the absorbance was about 0.5 at the excitation wavelength in a 2 mm optical path quartz cell. Sample solution was stirred by a Teflon-coated bar. To avoid rotational diffusion effects, the pump beam was depolarized by passing through an achromatic depolarizer. Whereas this will not eliminate rotational diffusion entirely as in the case of linearly polarized pump and probe at magic angle conditions,[46, 47] rotational diffusion of organic fluorophores of the size of **bn** is expected to be around 100-200 ps in low viscosity solvents as methanol and water,[48] and hence will not greatly affect the dynamics on the 0.3-30 ps time scale investigated. Control experiments were performed also at magic angle conditions (54.7° between excitation and probe polarizations) and gave similar results. The entire set of pump-probe delay positions was repeated at least four times, to ensure data reproducibility. The transient absorption data

were corrected for chirp of white light continuum. The data were analyzed by determination of the band integral kinetics and were fitted with a single-exponential function. The instruments response function (IRF) was about 200 fs (FWHM) in experiments with 475 and 535 nm excitations. IRF was 350 fs (FWHM) with the excitation at 287 nm. Convolution with a Gaussian response function was included in the global fitting procedure (ASUFIT program), satisfactory fits were obtained with $\Delta A(t) = A_1\exp(-t/\tau_1) + A_2\exp(-t/\tau_2) + A_3$.

Emission and excitation fluorescence spectra were recorded on a Horiba Jobin-Yvon-Spex Fluorolog 3-22 spectrofluorometer. Right-angle geometry was used for all steady state emission measurements. Simple emission and excitation spectra were determined with six replicates at a reduced scanning rate. The experiments were performed on 4 mL sample solutions contained in a quartz cell (1 cm × 1 cm) with **bn** absorbance not exceeding 0.1 at the excitation wavelength (1.5×10^{-6} M). The excitation wavelength was set at λ_{exc} = 530 nm. Fluorescence spectra were collected with 2 nm excitation and emission slits, using 0.5 s integration time. Stationary UV-vis absorption spectra were recorded using Jasco V-550 spectrophotometer.

Acknowledgments

This work was performed with financial support of the Polish National Science Centre (NCN), project DEC-2013/09/B/ST4/00273. Calculations were performed at the PL-Grid project.

Notes and references

[a] Quantum Electronics Laboratory, Faculty of Physics,
Adam Mickiewicz University in Poznan, Umultowska 85, 61-614 Poznan, Poland
E-mail: gotardb@amu.edu.pl

[b] Section of Analytical Chemistry, Faculty of Chemical Engineering and Technology,
Institute C-1, Cracow University of Technology, Warszawska 24, 31-155 Cracow, Poland

[c] Faculty of Chemistry, Adam Mickiewicz University in Poznan, Umultowska 89b, 61-614 Poznan, Poland

Electronic Supplementary Information (ESI) available: ultrafast transient spectra and kinetics and TD-DFT calculations, experimental details. See DOI:

References:

1. T. Esatbeyoglu, A. E. Wagner, V. B. Schini-Kerth and G. Rimbach, *Mol. Nutr. Food Res.*, 2015, **59**, 36.
2. F. C. Stintzing and R. Carle, *Trends Food Sci. Technol.*, 2004, **15**, 19.
3. D. Strack, T. Vogt and W. Schliemann, *Phytochem.*, 2003, **62**, 247.
4. S. Wybraniec, P. Stalica, A. Sporna and Y. Mizrahi, *J. Agric. Food Chem.*, 2010, **58**, 5347.
5. M. Ibdah, A. Krins, H. K. Seidlitz, W. Heller, D. Strack and T. Vogt, *Plant, Cell and Envir.*, 2002, **25**, 1145.
6. T. Vogt, M. Ibdah, J. Schemidt, V. Wray, M. Nimtz and D. Strack, *Phytochem.*, 1999, **52**, 583.
7. J. A. Bonacin, F. M. Engelmann, D. Severino, H. E. Toma and M. S. Baptista, *J. Braz. Chem. Soc.*, 2009, **20**, 31.
8. C. Sandquist and J. McHale, *J. Photochem. Photobiol. A: Chem.*, 2011, **221**, 90.
9. F. J. Knorr, D. J. Malamen, J. L. McHale, A. Marchioro and J.-E. Moser, *Proc. of SPIE*, 2014, **9165**, 91650N.
10. T. Kujala, J. Loponen and K. Pihlaja, *Z. Naturforsch.*, 2001, **56c**, 343.
11. J. Kanner, S. Harel and R. Granit, *J. Agric. Food Chem.*, 2001, **49**, 5178.
12. M. R. Moßhammer, F. C. Stintzing and R. Carle, *J. Prof. Assoc. Cactus Dev.*, 2006, **8**, 1.
13. S. Wybraniec and B. Nowak-Wydra, *J. Agric. Food Chem.*, 2007, **55**, 8138.
14. S. Wybraniec and Y. Mizrahi, *J. Agric. Food Chem.*, 2002, **50**, 6086.
15. L. C. P. Goncalves, M. A. S. Trassi, N. B. Lopes, F. A. Dorr, M. T. Santos, W. J. Baader, V. X. Oliviera Jr. and E. L. Bastos, *Food Chem.*, 2012, **131**, 231.
16. F. C. Stintzing, J. Conrad, I. Klaiber, U. Beifuss and R. Carle, *Phytochem.*, 2004, **65**, 415.
17. J. H. von Elbe and I.-V. Maing, *Cereal Sci. Today*, 1973, **18**, 263.
18. F. H. Bartoloni, L. C. P. Goncalves, A. C. B. Rodriguez, F. A. Dorr, E. Pinto and E. L. Bastos, *Monatsh. Chem.*, 2013, **144**, 567.
19. T. Nilsson, *Lantbruksh. Ann.*, 1970, **36**, 179.
20. K. M. Herbach, F. C. Stintzing and R. Carle, *J. Food Sci.*, 2006, **71**, R41.
21. E. L. Attoe and J. H. von Elbe, *J. Food Sci.*, 1981, **46**, 1934.
22. A. Skopinska, D. Tuwalska, S. Wybraniec, K. Starzak, K. Mitka, P. Kowalski and M. Szaleniec, *Chall. Modern Technol.*, 2012, **3**, 34.
23. S. J. Schwartz and J. H. von Elbe, *Agric. Food Chem.*, 1980, **28**, 540.
24. C. Qin and A. E. Clark, *Chem. Phys. Lett.*, 2007, **438**, 26.
25. C. L. Oprea, A. Dumbrava, I. Enache, A. Georgescu and M. A. Girtu, *J. Photochem. Photobiol. A: Chem.*, 2012, **240**, 5.
26. M. Piattelli and L. Minale, *Phytochem.*, 1964, **3**, 547.
27. M. Wendel, D. Szot, K. Starzak, D. Tuwalska, D. Prukala, T. Pedzinski, M. Sikorski, S. Wybraniec and G. Burdzinski, *Dyes Pigments*, 2015, **113**, 634.
28. D. Magde, R. Wong and P. G. Seybold, *Photochem. Photobiol.*, 2002, **75**, 327.
29. F. Gandia-Herrero, J. Escribano and F. Garcia-Carmona, *Planta*, 2010, **232**, 449.
30. A. C. B. Rodrigues, L. C. P. Goncalves and E. L. Bastos, *12th International Conference on Methods and Applications of Fluorescence, Strasbourg 2011, France*.
31. J. L. Perez-Lustres, F. Rodriguez-Prieto, M. Mosquera, T. A. Senyushkina, N. P. Ernsting and S. A. Kovalenko, *J. Am. Chem. Soc.*, 2007, **129**, 5408.

32. S. A. Kovalenko, R. Schanz, V. M. Farztdinov, H. Hennig and N. P. Ernsting, *Chem. Phys. Lett.*, 2000, **323**, 312.
33. S. A. Kovalenko, R. Schantz, H. Hennig and N. P. Ernsting, *J. Chem. Phys.*, 2001, **115**, 3256.
34. X. Tan, T. L. Gustafson, C. Lefumeux, G. Burdzinski, G. Buntinx and O. Poizat, *J. Phys. Chem. A*, 2002, **106**, 3593.
35. A. Rosspeintner, B. Lang and E. Vauthey, *Annu. Rev. Phys. Chem.*, 2013, **64**, 247.
36. A. Pigliucci, G. Duvanel, L. M. L. Daku and E. Vauthey, *J. Phys. Chem. A*, 2007, **111**, 6135.
37. M. L. Horng, J. A. Gardecki, A. Papazynan and M. Maroncelli, *J. Phys. Chem.*, 1995, **99**, 17311.
38. T. S. Kujala, M. S. Vienola, K. D. Klika, J. M. Loponen and K. Pihlaja, *Eur. Food Res. Technol.*, 2002, **214**, 505.
39. M. N. Gasztonyi, H. Daood, M. T. Hajos and P. Biacs, *J. Sci. Food Agric.*, 2001, **81**, 932.
40. S. Wybraniec, *J. Agric. Food Chem.*, 2005, **53**, 3483.
41. G. Jerz, T. Skotzki, K. Fiege, P. Winterhalter and S. Wybraniec, *J. Chromatogr. A*, 2008, **1190**, 63.
42. B. Nemzer, Z. Pietrzkowski, A. Sporna, P. Stalica, W. Thresher, T. Michalowski and S. Wybraniec, *Food Chem.*, 2011, **127**, 42.
43. A. Furstenberg and E. Vauthey, *Photochem. Photobiol. Sci.*, 2005, **4**, 260.
44. M. Sajadi, M. Weinberger, H.-A. Wagenknecht and N. P. Ernsting, *Phys. Chem. Chem. Phys.*, 2011, **13**, 17768.
45. C. T. Middleton, B. Cohen and B. Kohler, *J. Phys. Chem. A*, 2007, **111**, 10460.
46. H. E. Lessing and A. von Jena, *Chem. Phys. Lett.*, 1976, **42**, 213.
47. G. R. Fleming, in *Chemical applications of ultrafast spectroscopy*, ed. G. R. Fleming, Oxford University Press, New York, 1986, pp. 124.
48. G. B. Dutt, S. Doraiswamy, N. Periasamy and B. Venkataraman, *J. Chem. Phys.*, 1990, **93**, 8498.

Table 1. Fluorescence quantum yield Φ_f of betanin in aqueous and alcoholic solutions (λ_{exc} = 530 nm). The maxima of the initial betanin S_1 absorption band were observed in UV-vis-NIR transient absorption measurements (λ_{exc} = 535 nm). Time-constants τ_1 and τ_2 were deduced from global analysis. The betanin S_1 excited state lifetime τ_{S1} was obtained from the band integral.

solvent	viscosity [cP]	Φ_f	$\lambda_{S1\ abs}^{max}$ [nm]	τ_1 [ps]	τ_2 [ps]	τ_{S1} [ps]
water	0.89	0.0007	450, 1225	0.86	6.8	6.4
methanol	0.54	0.0013	445, 1235	1.6	9.4	7.7
ethylene glycol	16.1	0.0046	455, 1215	4.4	29.7	27

Figure 1. Chemical structure of betanin.

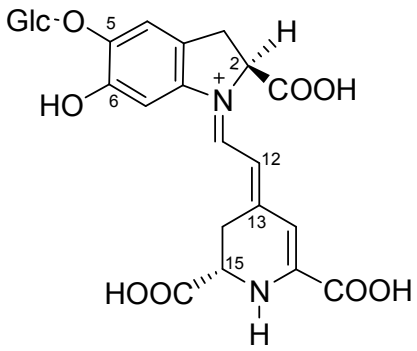

betanin

Figure 2. Stationary normalized UV-vis absorption and fluorescence spectra (λ_{exc} = 530 nm) for betanin in aqueous and alcoholic solutions.

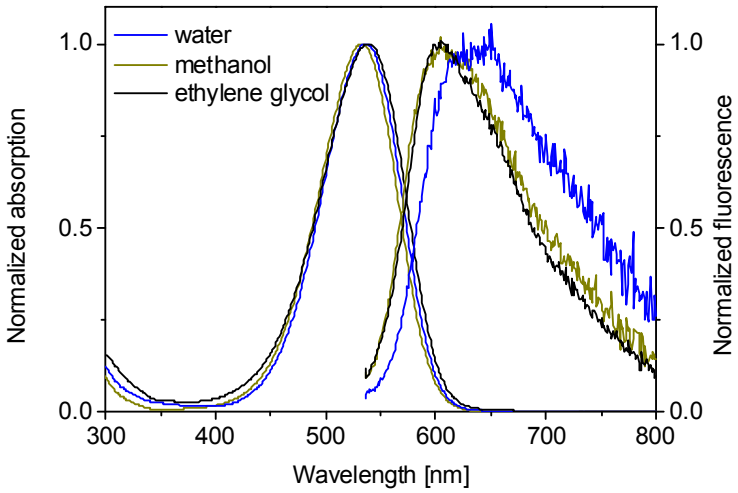

Figure 3. UV-vis-NIR transient absorption spectra recorded over a 0.3 – 30 ps time window following photoexcitation of betanin at 535 nm (4.8×10^{-5} M) in water (pH = 7.0). Stationary absorption spectrum and the emission cross-section spectrum of aqueous betanin solution. Jablonski diagram shows betanin S_1 deactivation paths.

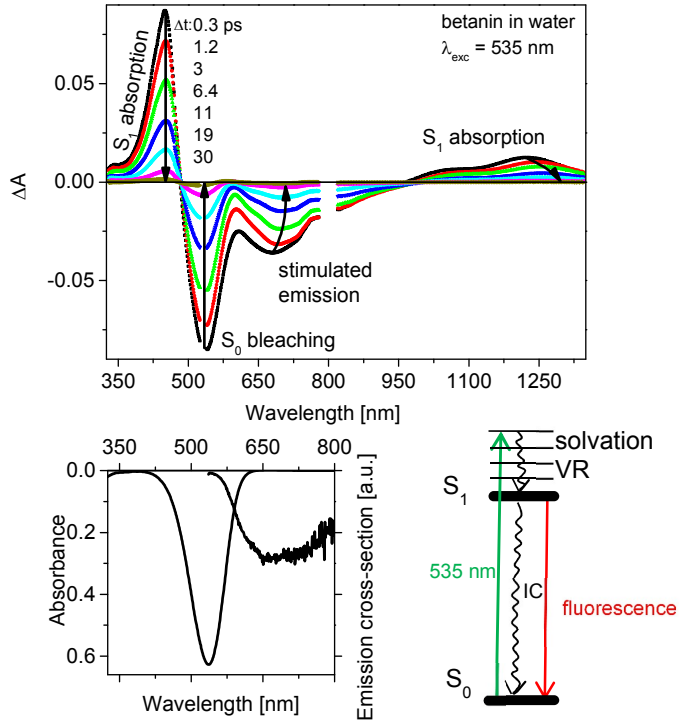

Figure 4. Normalized kinetic traces of the calculated band integrals for betanin in water, methanol and ethylene glycol.

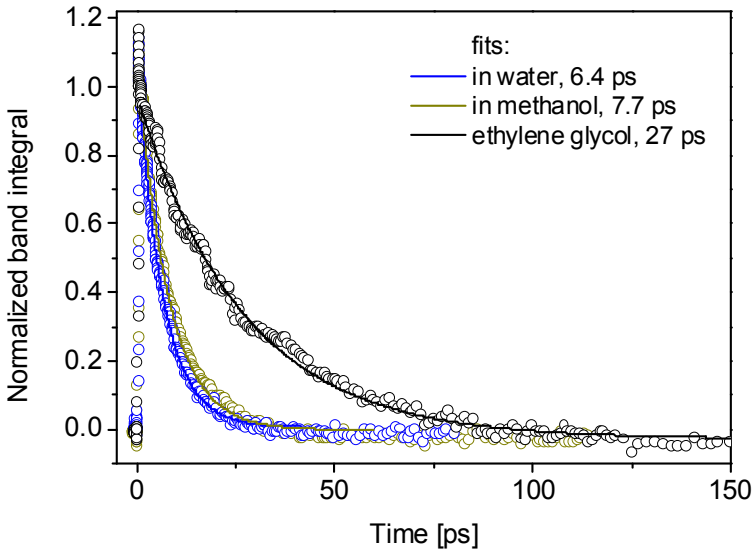

Figure 5. Transient absorption spectra recorded for betanin (4.8×10^{-5} M) in aqueous solution (A) and determined decay-associated spectra for the data recorded with the excitation at 287 nm (B). Selected kinetics at 450 nm and 535 nm (C) fitted with a single exponential function convoluted with IRF 350 fs FWHM.

(A)

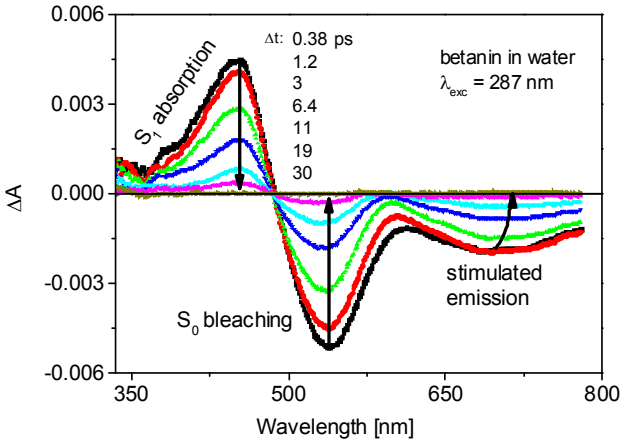

(B)

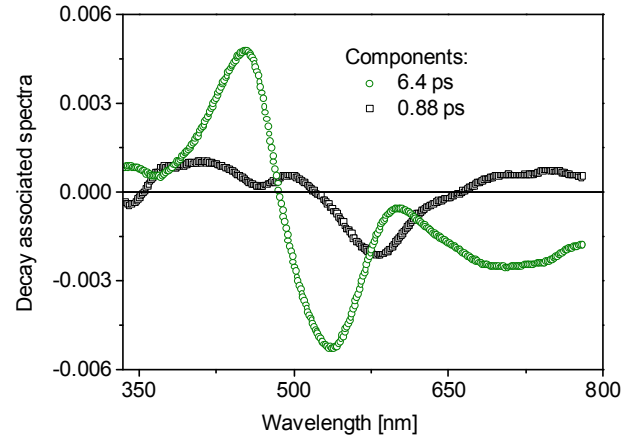

(C)